

Understanding the behavior of different metals in loaded scintillators: discrepancy between gadolinium and bismuth

Guillaume H.V. Bertrand, Jonathan Dumazert, Fabien Sguerra, Romain Coulon, Gwenolé Corre and
Matthieu Hamel*

Supporting information

Index

Experimental: radioluminescence	3
Table SI1: scintillation yields for each point on the PPO/Bi graph with a ^{137}Cs source	3
Table SI2: scintillation yields for each point on the PPO/Gd graph with a ^{137}Cs source	4
Figure Si1: Evolution of scintillation yields with various PPO and bismuth concentration. series A to E with a ^{241}Am source	5
Figure Si2: Evolution of scintillation yields with various PPO and bismuth concentration. series A to E with a ^{22}Na source	5
Figure Si3: Evolution of scintillation yields with various PPO and gadolinium concentration. series F to J with a ^{241}Am source	6
Figure SI4: Evolution of scintillation yields with various PPO and gadolinium concentration. series F to J with a ^{22}Na source	6
Figure SI5: left. Photo of sample K. 5 wt% bismuth loaded plastic scintillator; right UV response.....	7
Figure SI6: emission spectra of sample K. 5 wt% bismuth loaded plastic scintillator	7
Figure SI7: radioluminescence of sample K. 5 wt% bismuth loaded plastic scintillator under beta irradiation (90Sr/90Y)	8
Figure SI8: Mean pulse for decay time measurements of sample K. 5 wt% bismuth loaded plastic scintillator.....	9
Figure SI9: Pulse height spectra of EJ256-5 wt% lead loaded (black) and sample K. 5 wt% bismuth loaded (red) plastic scintillators with a ^{57}Co source	9
Figure SI10: Pulse height spectra of EJ256-5 wt% lead loaded (black) and sample K. 5 wt% bismuth loaded (red) plastic scintillators with a ^{137}Cs source	10
Figure SI11: emission spectra of sample L. 2 wt% gadolinium loaded plastic scintillator	10
Figure SI12: radioluminescence of sample L. 2 wt% gadolinium loaded plastic scintillator under beta irradiation (90Sr/90Y)	11
Figure SI13: Mean pulse for decay time measurements of sample L. 2 wt% gadolinium loaded plastic scintillator.....	11

Experimental: radioluminescence.

Radioluminescence spectra were acquired by using the following procedure. In the Fluoromax 4P spectrofluorometer (Horiba), the excitation light was shut down. In the center of the experimenter chamber, $^{90}\text{Sr}/^{90}\text{Y}$ β -emitting source (25 MBq) was placed at 1 cm away from the scintillator to irradiate the plastic scintillator located close to the detection cell. Spectra were acquired with integration time 5 s/nm. Two types of blank spectra were recorded: one with the plastic scintillator without source and one with the source without scintillator, in order to establish a base line. Plastic scintillator EJ-200 was purchased from Eljen Technology and was used as reference set at 10,000 ph/MeV.

	1		2		3		4		5	
	wt% PPO	Scintillation yields for 0 wt% Bi	wt% PPO	Scintillation yields for 1 wt% Bi	w% PPO	Scintillation yields for 2 wt% Bi	wt% PPO	Scintillation yields for 5 wt% Bi	w% PPO	Scintillation yields for 10 wt% Bi
A	0.5	--	0.5	0.55	0.5	0.43	0.5	0.25	0.5	0.09
B	1	--	1	--	1	0.61	1	0.30	1	0.14
C	3	0.79	3	0.77	3	0.68	3	0.39	2	0.16
D	9	0.90	9	0.84	9	0.73	8	0.49	8	0.21
E	23	1.00	23	0.93	22	0.85	21	0.69	20	0.35

Table SI1: scintillation yields for each point on the PPO/Bi graph with a ^{137}Cs source

	1		2		3		4	
	PPO wt%	Scintillation yields for 0 wt% Gd	PPO w%	Scintillation yields for 1 wt% Gd	PPO wt%	Scintillation yields for 2wt% Gd	PPO wt%	Scintillation yields 2 for wt% Gd
F	0.5	--	0.5	0.37	0.5	0.21	0.4	0.10
G	1	0.89	1	0.60	1	0.31	1	0.10
H	3	0.90	3	0.73	3	0.49	2	0.12
I	9	0.97	9	0.69	8	0.45	8	0.17
J	23	1.00	22	0.71	22	0.49	20	0.17

Table SI2: scintillation yields for each point on the PPO/Gd graph with a ^{137}Cs source

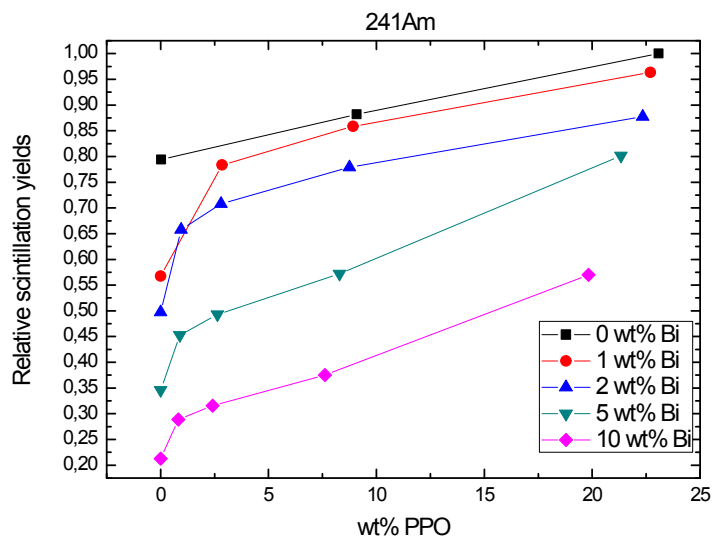


Figure Si1: Evolution of scintillation yields with various PPO and bismuth concentration. series A to E with a ^{241}Am source

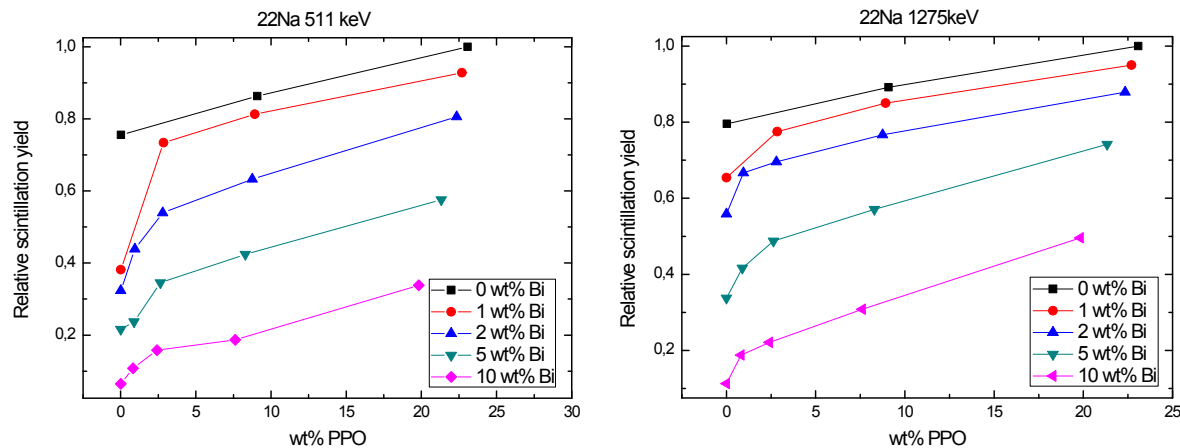


Figure Si2: Evolution of scintillation yields with various PPO and bismuth concentration. series A to E with a ^{22}Na source

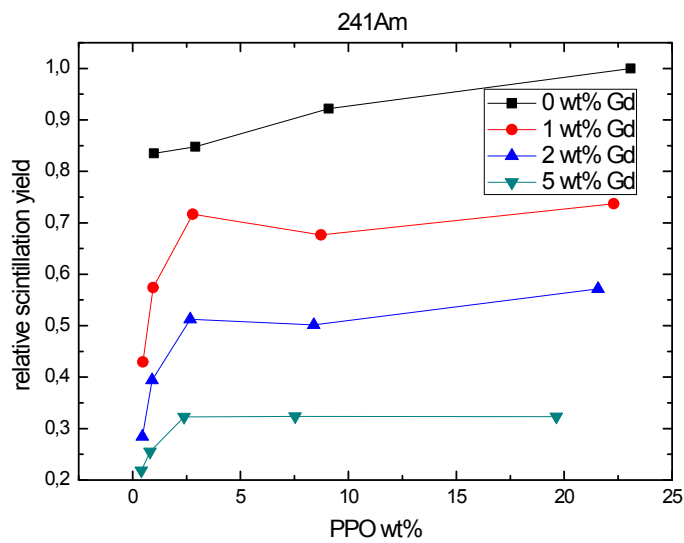


Figure Si3: Evolution of scintillation yields with various PPO and gadolinium concentration.
series F to J with a ^{241}Am source

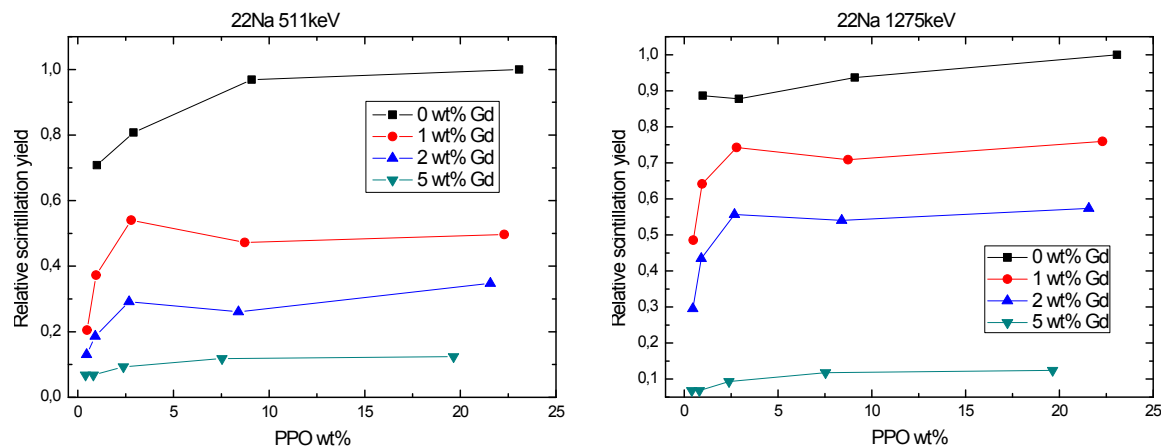


Figure Si4: Evolution of scintillation yields with various PPO and gadolinium concentration.
series F to J with a ^{22}Na source

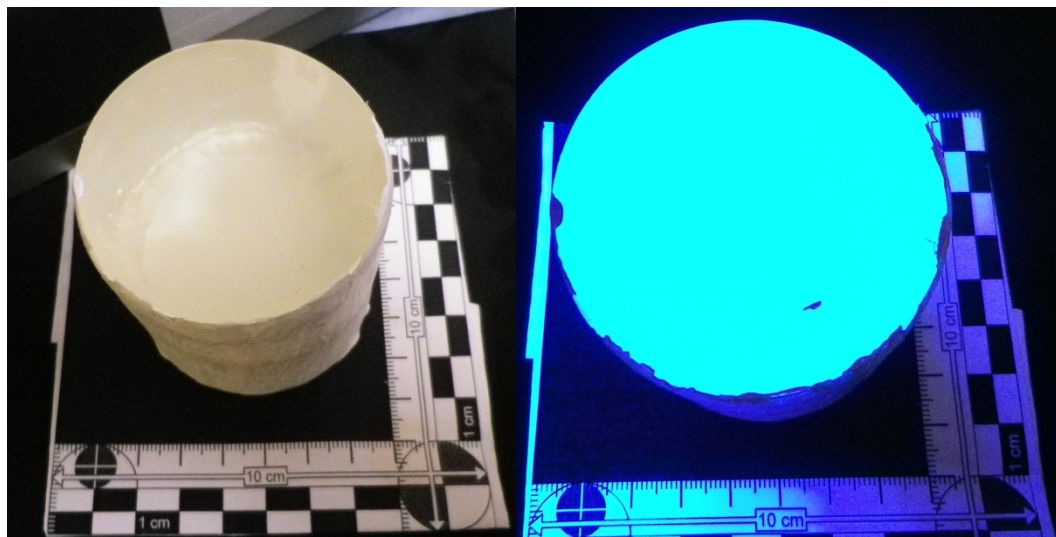


Figure SI5: left. Photo of sample K. 5 wt% bismuth loaded plastic scintillator; right UV response.

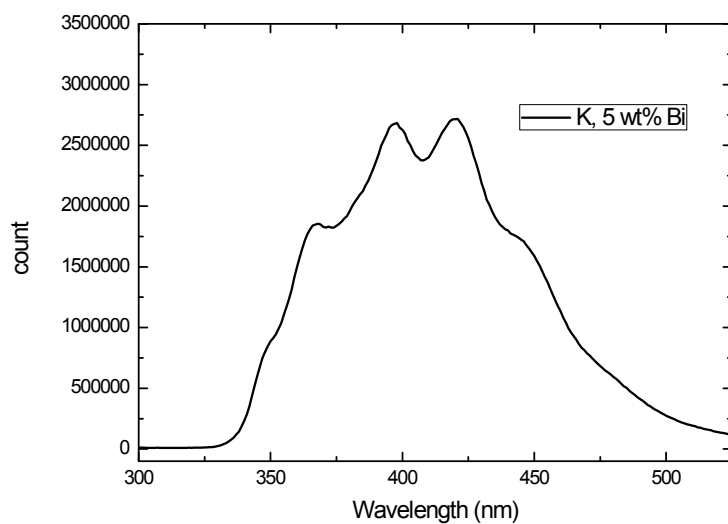


Figure SI6: emission spectra of sample K. 5 wt% bismuth loaded plastic scintillator

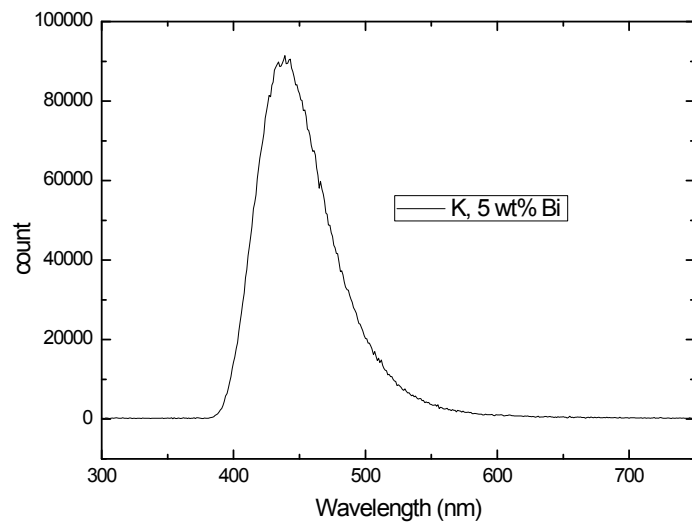


Figure SI7: radioluminescence of sample K. 5 wt% bismuth loaded plastic scintillator under beta irradiation ($^{90}\text{Sr}/^{90}\text{Y}$)

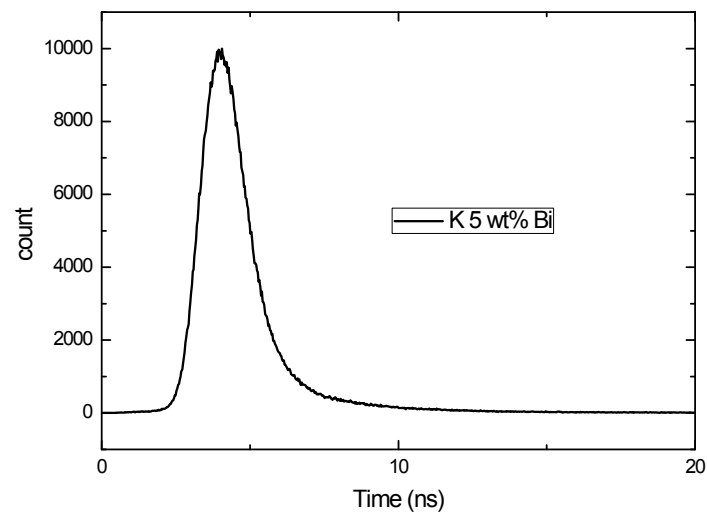


Figure SI8: Mean pulse for decay time measurements of sample K. 5 wt% bismuth loaded plastic scintillator

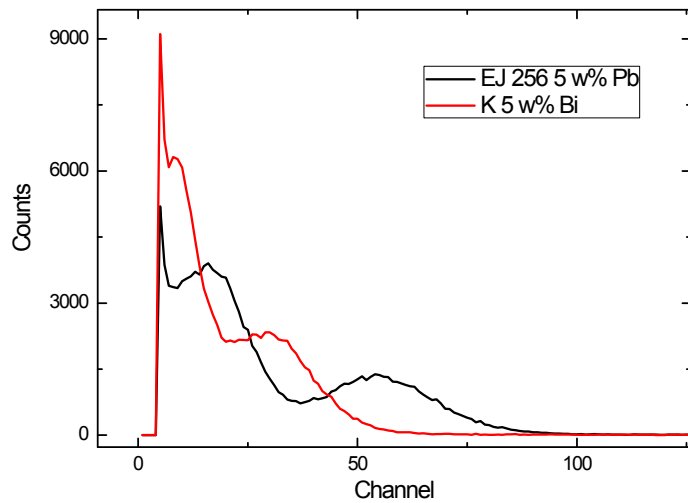


Figure SI9: Pulse height spectra of EJ256-5 wt% lead loaded (black) and sample K. 5 wt% bismuth loaded (red) plastic scintillators with a ^{57}Co source

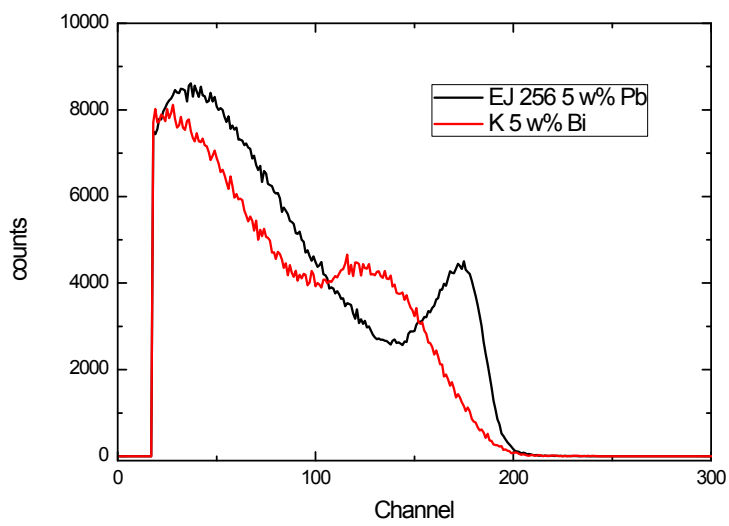


Figure SI10: Pulse height spectra of EJ256-5 wt% lead loaded (black) and sample K. 5 wt% bismuth loaded (red) plastic scintillators with a ^{137}Cs source

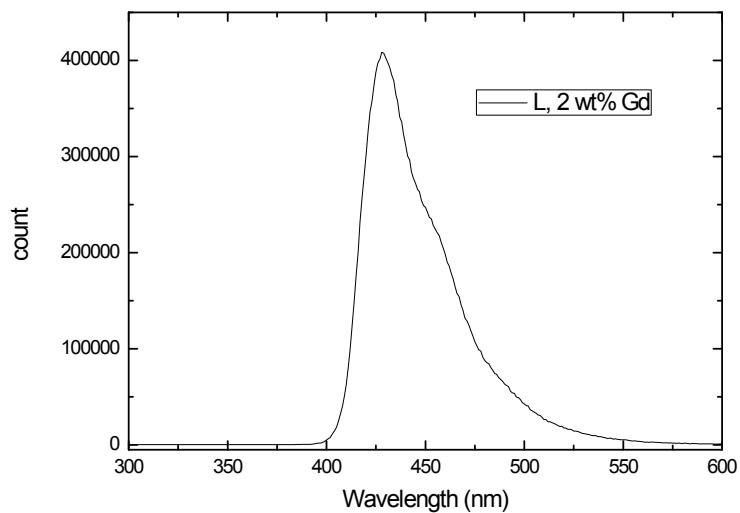


Figure SI11: emission spectra of sample L. 2 wt% gadolinium loaded plastic scintillator

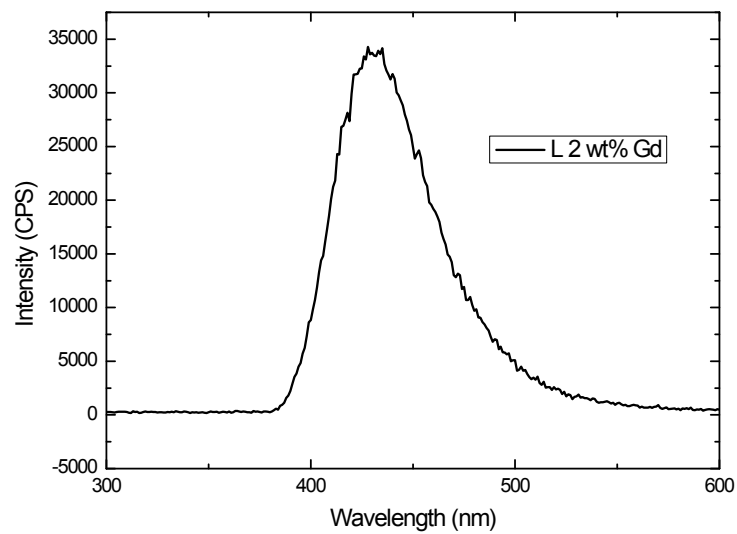


Figure SI12: radioluminescence of sample L. 2 wt% gadolinium loaded plastic scintillator under beta irradiation (90Sr/90Y)

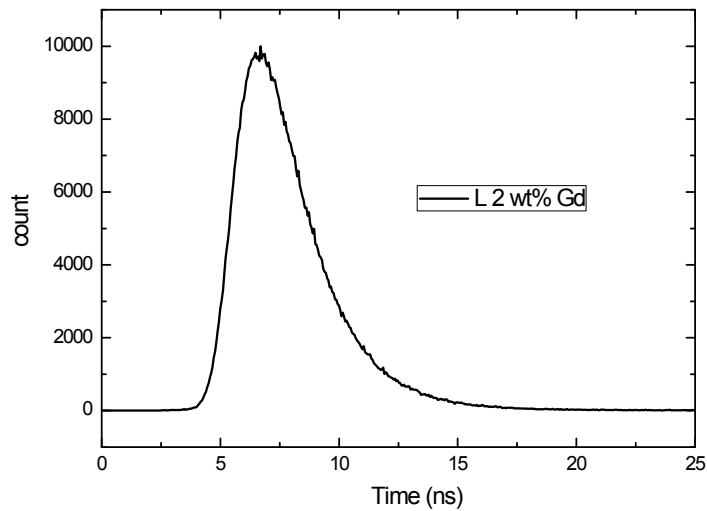


Figure SI13: Mean pulse for decay time measurements of sample L. 2 wt% gadolinium loaded plastic scintillator